J Therm Anal Calorim (2010) 99:609–619
DOI 10.1007/s10973-009-0001-z

A combined approach of differential scanning calorimetry and hot-stage microscopy with image analysis in the investigation of sulfathiazole polymorphism

Mohd Rushdi Abu Bakar · Zoltan Kalman Nagy · Christopher David Rielly

Received: 18 February 2009 / Accepted: 7 May 2009 / Published online: 6 August 2009

Abstract A combination of differential scanning calorimetry and hot-stage microscopy with image analysis has been used to investigate the polymorphism of sulfathiazole. The use of light intensity profiles obtained from the HSM images, as an alternative way to present results of the HSM analysis, was found to be useful in describing and verifying thermal events. The approach provides a unique insight into the polymorphic transformations and thermal behaviour exhibited by this compound. The results of the experiments show that sulfathiazole tends to crystallise as mixtures of polymorphs, even though the literature methods for producing pure polymorph were followed.

Keywords DSC · HSM · Image processing · Polymorphic transformation

Introduction

Crystallisations of active pharmaceutical ingredients (APIs) particularly those that possess multiple polymorphic forms are amongst the most critical, yet least understood pharmaceutical processes. Statistically, about 85% of APIs exhibit polymorphism and 50% have multiple polymorphic forms [1]. The polymorphs of a crystal can exhibit a variety of structures, which have different inter- and intra-molecular interactions. Thus, they have different free energies and consequently different physico-chemical properties and mechanical behaviours [2]. These have an impact on downstream process operations, such as isolation, filtering and drying, and can affect the therapeutic properties of the final product. For this reason, an extensive characterisation of all known solid forms of the API is necessary in order to understand and differentiate them properly. Solid state characterisation has become an integral part of the drug development process and its importance has been recognised from scientific as well as regulatory concerns. It has been used to provide information about the therapeutic properties of the polymorphs of a drug substance such as their bioavailability, rate of dissolution and stability. It also has been used to assess the success of the crystallisation control approach in producing certain polymorphs [3, 4] and certain crystal properties [5–7]. In addition, the obtained knowledge on the solid state properties of the API could assist in generating a valuable protection of intellectual property, e.g., through a patent [2].

Thermal analysis is one of the established solid state characterisation techniques. Its application to characterise pharmaceutical products has been extensively reviewed in the literature [8–12]. One of the most widely used thermal analysis techniques for the investigation of polymorphism is differential scanning calorimetry (DSC). The technique basically involves the application of a heating/cooling signal to a sample and the subsequent measurement of the temperature and enthalpy changes associated with thermal events such as melting and polymorphic transformation [13]. The popularity of DSC is due to its simplicity and rapidity of measurement, requirement for a small sample size and ability to provide detailed information about the physical and energetic properties of a sample [14].

Another thermal analysis technique for the investigation of polymorphism is hot-stage microscopy (HSM). The technique combines microscopy and thermal analysis, and allows visual observation of the behaviour of a sample through a microscope during heating or cooling [15]. This

M. R. Abu Bakar · Z. K. Nagy (✉) · C. D. Rielly
Department of Chemical Engineering, Loughborough University, Loughborough, Leicestershire LE11 3TU, UK
e-mail: Z.K.Nagy@lboro.ac.uk

visual technique easily distinguishes a polymorphic transformation from the melting process [16]; hence HSM is very useful to provide information for the confirmation of the thermal events that are observed using other techniques. Some examples of the application of HSM in the thermal analysis of pharmaceuticals have been comprehensively presented by Vitez and Newman [17]. Recent technological advances have expanded the capabilities of the visual techniques, for example with the use of software, which not only captures the image, but also performs an image analysis, for example by computing the total light intensity. The latter may be calculated as the sum or average of the grey levels in all pixel (pixel value ranges from black = 0 to white = 255). As the image becomes brighter, the light intensity value becomes higher. The application of image analysis to evaluate HSM results is very attractive because of its ability to translate visual effects, which other techniques may not be able to provide, into quantitative information. The introduction of an alternative way of presenting HSM results may broaden the application of HSM since it is conventionally used to confirm results of other thermal analysis techniques only. Some visual techniques, including optical microscopy, non-invasive video imaging systems and Lasentec's in-process video microscopy, have successfully utilized image analysis in the investigation of the dynamics of product quality, such as size and shape of particulates in real-time and in situ [18–22]. However, based on authors' knowledge, the use of image analysis to evaluate HSM results has never been reported.

Although solid state properties of different polymorphs of a compound may be different, very often, they are only marginally different. For this reason, it is essential to differentiate them using a variety of characterisation techniques to avoid making erroneous conclusions. In addition, the interpretation of an individual characterisation technique always requires support from other techniques. A reliable combined technique that can quickly differentiate between different polymorphs and determine if a solid contains a pure polymorph or a mixture of polymorphs would be preferable. Combined or coupled thermal analysis techniques were found to provide quicker ways for interpretation of polymorphic phenomena, while at the same time, the sensitivity, the reliability and the robustness of the results remain of high quality [23, 24]. This is illustrated by a coupling of DSC and HSM, which have proved to be very successful in the study of phase diagrams and polymorphic transformation [25–28]. Based on their works, visual observation through HSM was found to be a more sensitive indicator of phase changes than the DSC measurements alone; the changes happening on the surface of the crystals could clearly be seen using HSM even when the DSC showed no thermal event [26]. Very recently, a DSC coupled to a photovisual system (i.e., a microscopy connected to a camera) has been employed to confirm the presence of volatile solvents in raw materials of indinavir sulphate, which was shown by liberation of bubbles during volatilization process upon heating [29].

Sulfathiazole has been chosen as the model system in this study. At present, it has five known polymorphs that are well characterised and clearly described in the literature [30–32]. Although the polymorphism of sulfathiazole has been extensively and repeatedly investigated by various researchers [33–36], it remains difficult to produce a pure polymorph; most of the time, the desired polymorph contains impurities from at least one other form [37–40].

In this paper, examples are presented of complementary application of DSC and HSM with image analysis in the investigation of sulfathiazole polymorphism. The image analysis tool used in this work allows the selection of regions of interest and restricts image analysis to each selected region only. The aim of this work is two-fold: (i) to give a contribution to the methods of investigating polymorphism through a combined approach of DSC-HSM with image analysis, and (ii) to gain more understanding on the polymorphism of sulfathiazole.

Methods and materials

Materials

Sulfathiazole was purchased from Sigma-Aldrich with a purity of 98%. The solvents used are deionised water, 1-propanol, acetone and chloroform. Except water, all other solvents were analytical reagent grade purchased from Fisher Scientific.

Crystallisation of the polymorphs

Four different sulfathiazole polymorphs were generated using methods available in the literature [34, 38, 41] as shown in Table 1. One of the polymorphs (i.e., form II) was generated using two different methods. It is known that there are some inconsistencies in the enumeration of the sulfathiazole polymorphs in the literature [30, 42]. In this work, the enumeration of the polymorphs follows the convention proposed by Apperley and co-researchers [30]. In order to further clarify the identity of the polymorphs, the Cambridge Structural Database (CSD) reference codes are quoted in the bracket.

All of the crystallised solids were vacuum filtered and subsequently, those crystals obtained from water, were immediately dried in a hot air oven at 105 °C for 15 min, whereas crystals obtained from other solvents were dried in a desiccator.

Table 1 Preparation methods to produce different polymorphs of sulfathiazole

Method no.	Polymorph to be produced	Procedure
1	I (SUTHAZ01)	Heating 0.5 g of sulfathiazole in 50 mL of 1-propanol in a flask on a hot plate to dissolution, followed by natural cooling at 25 °C
2	II (SUTHAZ05)	Rapid cooling of a saturated aqueous solution of sulfathiazole at 60 °C (0.5 g in 100 mL water) from 80C to 4 °C at a set rate of 10 °C min^{-1} in a crystalliser
3	III (SUTHAZ02)	Slow cooling of a saturated aqueous solution of sulfathiazole (0.5 g in 100 mL water) at a rate of 0.1 °C min^{-1} from 80 to 20 °C in a crystalliser
4	IV (SUTHAZ)	Natural cooling to 20 °C a saturated solution of sulfathiazole in a 50:50 mixture of acetone: chloroform at 50 °C (1.3 g in 100 mL)
5	II (SUTHAZ05)	Boiling to evaporate a saturated aqueous solution of sulfathiazole at 60 °C (0.8 g in 50 mL water) in a beaker on a hot plate until almost dry

Thermal analysis of polymorphs

DSC: The thermal behaviour of the polymorphs was examined using a TA Instruments DSC Q10. About 8 mg of sample was weigh into an aluminium pan and sealed hermetically. Analysis was carried out by heating the sample from 100 to 240 °C at heating rates of 2, 10 and 20 °C min^{-1} under constant purging of nitrogen at 40 mL min^{-1}. An empty aluminium pan was used as a reference in all the runs. Results were analysed using TA Instruments Universal Analysis 2000.

HSM: The thermal behaviour of the polymorphs was visually examined using a Mettler Toledo FP90 hot-stage system and a Leica DMLM microscope from 100 to 250 °C at a heating rate of 10 °C min^{-1}. Microscopic observations during experiments were displayed on a computer screen and recorded using a JVC colour video camera.

HSM image analysis

MATLAB image processing toolbox (Matworks, Inc.) was used to compute mean values of light intensity of greyscale images in the HSM video clips. The computation was based on the average of grey levels in all pixel (pixel value ranges from black = 0 to white = 255). An algorithm for the computation is presented as a flowchart in Fig. 1. In this paper, the mean light intensity values of the HSM greyscale images is presented as percentage HSM light intensity, defined as a percentage of an average greyscale intensity value divided by the largest value of average greyscale intensity.

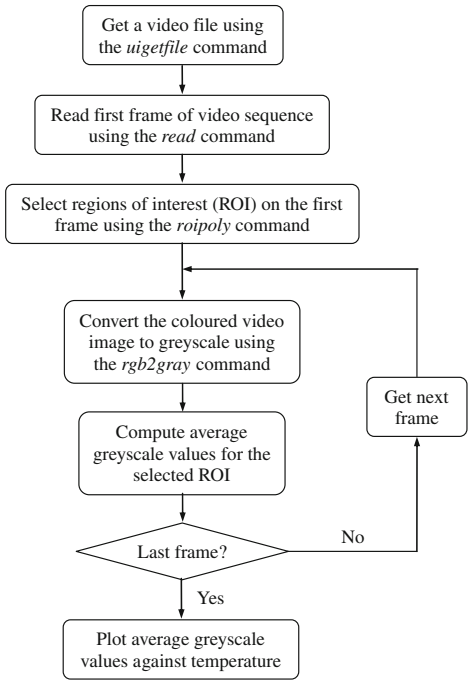

Fig. 1 An algorithm for the computation of mean light intensity values of greyscale images in the HSM video clips

Results and discussion

Crystals obtained by method 1

The DSC curves of the crystals obtained by method 1 at various heating rates are presented in Fig. 2. The onset of the first peak was observed between 121 and 131 °C, with the peak maxima increased from 124 to 136 °C, with increasing heating rates. The shifting of the onset of the peak and the peak maximum to higher temperatures as the heating rate increases is due to the effect of "thermal lag" within the system. The effect comes about as the result of the thermal lag between the DSC's furnace and the bottom of the sample pan, and/or the lag between the bottom of the sample pan and the sample, and/or the lag throughout the sample [43]. Therefore, although the use of a higher heating rate will reduce the experimental time, the thermal lag may affect the accuracy of the results. It can also be

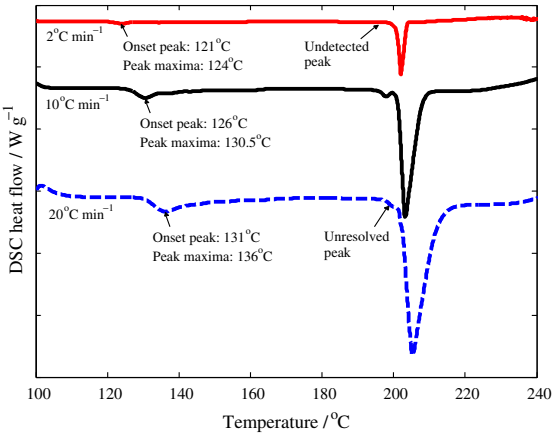

Fig. 2 DSC curves of sulfathiazole crystals obtained by method 1 at various heating rates

observed from Fig. 2 that the baseline of the curves is increasingly offset with an increase in the heating rate. The height and width of the peak are also increased, which consequently increased the detection limit, but reduced the resolution as demonstrated by the appearance of an unresolved peak for the run at a heating rate of 20 °C min^{-1}, whereas for the run at a heating rate of 2 °C min^{-1}, the peak is undetected. In order to compromise with all these effects, a heating rate of 10 °C min^{-1} was chosen for the subsequent thermal analysis experiments.

Figure 3 shows the DSC curve and the HSM light intensity of the crystals, while Fig. 4 shows the snapshots of selected crystals during HSM analysis. Both experiments, DSC and HSM, were conducted at a heating rate of 10 °C min^{-1}. Based on the DSC curve in Fig. 3, it can be seen that there are three major peaks. The peak with a maximum at 203.2 °C corresponds to the melting peak of form I, while the peak at a maximum of 197.9 °C corresponds to the melting peak of form II. Form I and form II

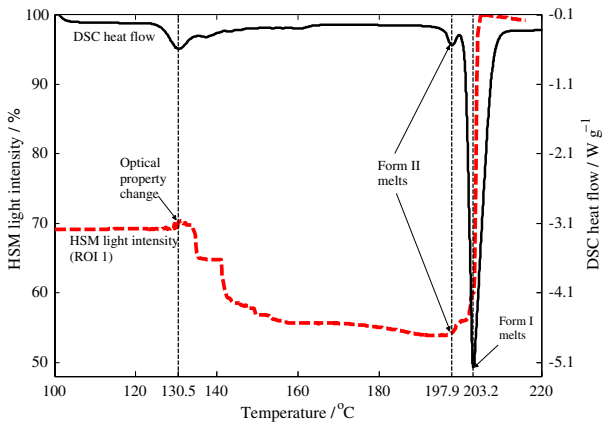

Fig. 3 DSC curve and HSM light intensity of sulfathiazole crystals obtained by method 1

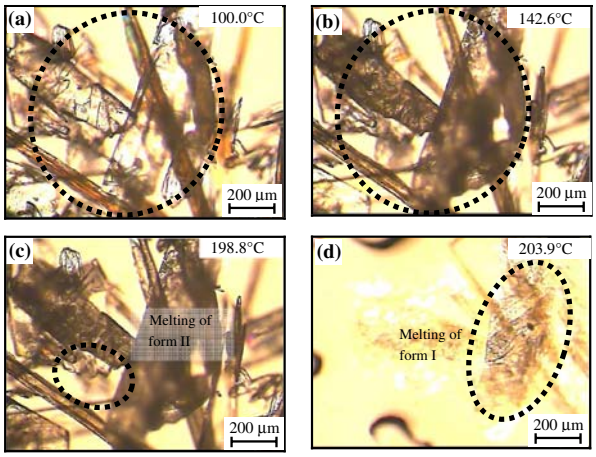

Fig. 4 Images of sulfathiazole crystals obtained by method 1 during HSM analysis taken at **a** 100.0 °C; **b** 142.6 °C; **c** 198.8 °C; and **d** 203.9 °C

are enantiotropically related, in which form I is stable from its melting point of 202 °C down to 116.5 °C, while form II is a stable form below 116.5 °C [44]. Some crystals of form I may have transformed into form II at room temperature during storage and when they were heated in the DSC experiment, some of them transformed back into form I. The formation of the peak at the maximum of 130.5 °C may correspond to a polymorphic transformation from form II to form I. The thermal lag effect mentioned earlier may have contributed to the difference between the obtained transition temperature at 130.5 °C and that from the literature at 116.5 °C [44]. These events, which were implied by the results of the DSC analysis, were verified by the HSM analysis. HSM shows no melting at the expected polymorphic transformation peak at 130.5 °C, but it shows an optical property change, as can be observed by the difference between the highlighted crystals in Fig. 4a and b. The change reduced the brightness and thus the light intensity of the crystals as indicated in Fig. 3 by the reduction in the HSM light intensity from 130.5 °C onwards. The same visual observation through a HSM had been reported in the case of lithium sulphate salt in which a transformation of one of its polymorphs to another was accompanied by a striking change in birefringence [45]. Melting of form II was indicated by a small increase in the value of the light intensity, while melting of form I was shown by the continuous increase in the value of the light intensity as all the crystals have melted. Figure 4 shows the melting of form II and form I in (c) and (d), respectively.

The profile of the HSM light intensity shown in Fig. 3 was computed from all crystals on the frame (ROI 1), which is fairly comparable to the profile of the sample's DSC curve. In order to investigate the capability and sensitivity of the HSM light intensity in describing thermal

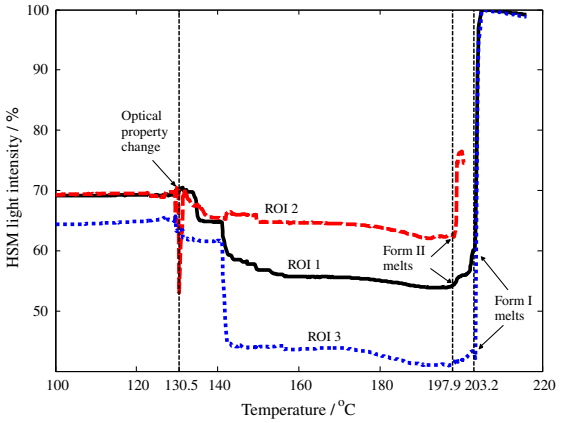

Fig. 5 HSM light intensity profiles of sulfathiazole crystals obtained by method 1 at three different ROIs; all crystals on the frame (ROI 1); a crystal that melts at 197.9 °C (ROI 2) and a crystal that melts at 203.2 °C (ROI 3)

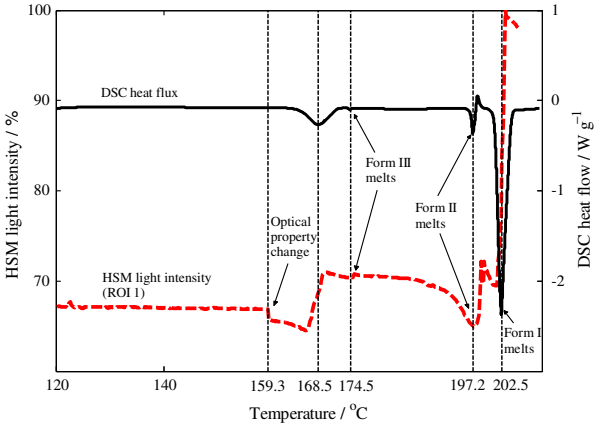

Fig. 6 DSC curve and HSM light intensity of sulfathiazole crystals obtained by method 2

events of individual crystals, two ROI were selected; one was selected around a crystal that melts at 197.9 °C (ROI 2) and another around a crystal that melts at 203.2 °C (ROI 3), as highlighted in Fig. 4c and d, respectively. The computed profiles of light intensity are shown in Fig. 5. It can be seen that all profiles indicate an optical property change with a decrease in the light intensity from 130.5 °C onwards. The profile of ROI 3, however, shows a larger decrease in the light intensity compared to the profile of ROI 2, but this is believed to be due to the difference in the appearance of the images since ROI 2 is more blurred than ROI 3. The absolute changes in the HSM light intensity depend on the fraction of ROI pixels that are filled with the crystal. The ROI 2 and ROI 3 profiles show the melting of crystals at 197.9 °C and 203.2 °C, respectively, with a sharp increase in the light intensity. The ROI 3 profile also shows a small peak that corresponds to the melting of a crystal in ROI 2, which demonstrates the sensitivity of the HSM light intensity to the changes happening on the surface of the crystals due to the melting of adjacent crystals. The results of DSC and HSM with image analysis show that the sulfathiazole crystals obtained by method 1 contain a mixture of form I and form II.

Crystals obtained by method 2

Figure 6 shows the profiles of the DSC curve and the HSM light intensity of the crystals produced by method 2. Figure 7 shows the snapshots of the crystals during HSM analysis. Based on Fig. 6, the DSC curve indicates the presence of three major endotherm peaks. The first peak at a maximum of 168.5 °C was not a melting peak as verified by the HSM analysis. The peak resulted from a change in the optical properties of the crystals, as shown by the

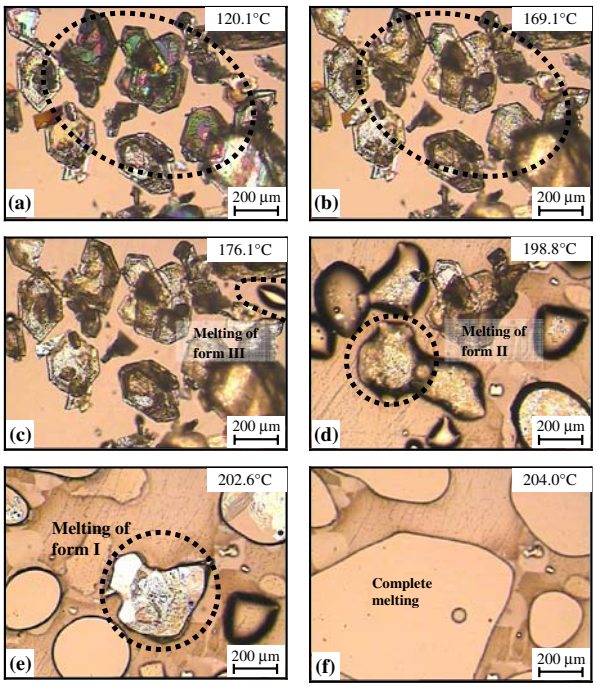

Fig. 7 Images of sulfathiazole crystals obtained by method 2 during HSM analysis taken at **a** 120.1 °C; **b** 169.1 °C; **c** 176.1 °C; **d** 198.8 °C; **e** 202.6 °C and **f** 204.0 °C

difference in the appearance of the highlighted crystals between (a) and (b) in Fig. 7. The phenomenon was indicated by fluctuation in the HSM light intensity profile between 159.3 °C to a temperature slightly above 168.5 °C and it was probably due to a transformation of form III to form I, since the transformation was reported to occur in a temperature range of 150–170 °C [34]. The second peak at

a maximum of 197.2 °C on the DSC curve corresponds to a melting peak of form II, whilst the third peak at a maximum of 202.5 °C corresponds to a melting peak of form I. The melting of form II and form I were verified by HSM analysis as shown in Fig. 7d and e, respectively, and the subsequent increase in the HSM light intensity value at the corresponding melting temperatures in Fig. 6. The HSM analysis was able to detect melting of form III as shown in Fig. 7c and as indicated in Fig. 6 by a small increase in the HSM light intensity value at 174.5 °C. This melting of form III was barely detected by the DSC. According to a report [35], a single melting peak of form II at its melting temperature can only be obtained if the crystals were purely form II. If only the slightest amount of form I present, form I will crystallise during the melting process of form II [35]. This indicates that the crystals obtained are actually a mixture of form I, form II and form III.

The HSM light intensity profiles for various ROI were presented in Fig. 8. ROI 2 was selected to represent a crystal that melts at 174.5 °C as highlighted in Fig. 7c, ROI 3 represents crystals that melt at 197.2 °C as shown in Fig. 7d and ROI 4 represents a crystal that melts at 202.5 °C as shown in Fig. 7e. All profiles show a sharp increase in the light intensity at the corresponding melting temperatures of their represented crystals. Although there are some discrepancies between the value of temperatures to represent melting at inflection points shown by the HSM light intensity and the DSC heat flux peak maximum, the relative errors are very small, i.e., between 0.1% and 0.7%. The fluctuation of the HSM light intensity profile between 159.3 and 169.4 °C that corresponds to the change in the optical properties of the crystals was shown by ROI 3 and ROI 4, but it was not shown by ROI 2. This result confirms that the phenomenon shown by the crystal in ROI 4 between 159.3 and 169.4 °C was due to a transformation of form III to form I. A similar phenomenon displayed by a crystal in ROI 2, on the other hand, was probably just due to a surface property change, since the crystal should not undergo a polymorphic transformation as it melted at its melting temperature of 197.2 °C (corresponding to melting temperature of form II crystals). Nevertheless, the HSM light intensity profiles of individual crystals in this case have been demonstrated to help in confirming the presence of form I, form II and form III in the crystals obtained by method 2.

Crystals obtained by method 3

The obtained DSC curve and the HSM light intensity for the sulfathiazole crystals from method 3 are presented in Fig. 9. Three endotherm peaks were shown by the DSC curve. The first peak had a maximum of 121 °C, the second at 162 °C and the third at 203.5 °C. The third peak corresponds to the melting peak of form I. The formation of the second peak is in agreement with the observation by previous researchers [34], who deduced that form III transforms into form I in the temperature range of 150–170 °C without showing any melting (of form III at 175 °C). This polymorphic transformation event implied by the results of the DSC analysis was confirmed by the HSM analysis. No melting, but a change in optical property of the crystals, was observed as shown by the difference between the highlighted crystals in Fig. 10a and b. The formation of the first peak lies within a range of temperatures that recently reported to correspond to the dehydration of a hydrate [46]. The HSM analysis confirmed this by showing no thermal event in the vicinity of 121 °C. This

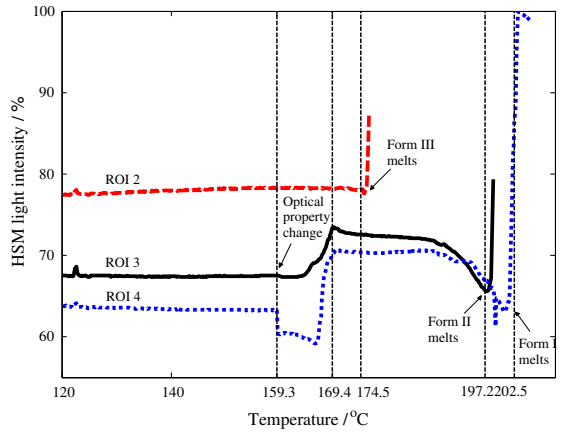

Fig. 8 HSM light intensity profiles of sulfathiazole crystals obtained by method 2 at three different ROIs; a crystal that melts at 174.5 °C (ROI 2); crystals that melt at 197.2 °C (ROI 3) and a crystal that melts at 202.5 °C (ROI 4)

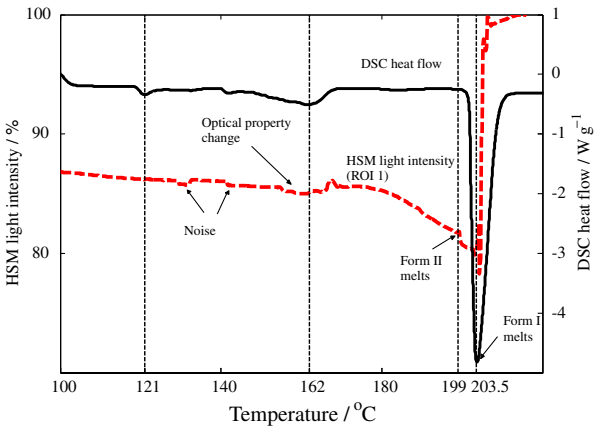

Fig. 9 DSC curve and HSM light intensity of sulfathiazole crystals obtained by method 3

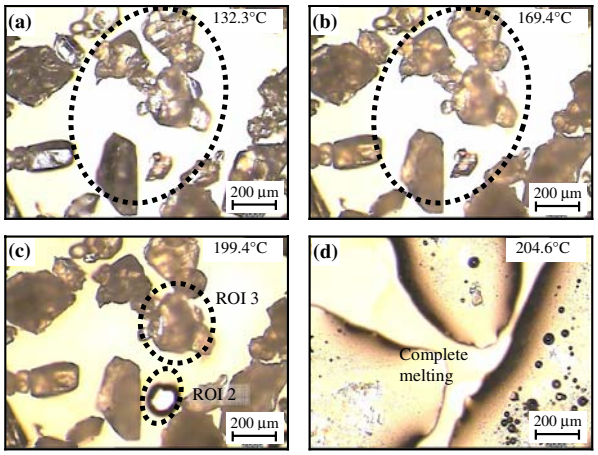

Fig. 10 Images of sulfathiazole crystals obtained by method 3 during HSM analysis taken at **a** 132.3 °C; **b** 169.4 °C; **c** 199.4 °C; and **d** 204.6 °C

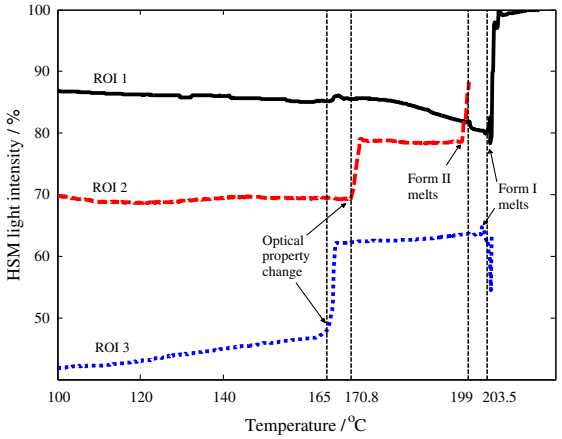

Fig. 11 HSM light intensity profiles of sulfathiazole crystals obtained from method 3 at three different ROIs; all crystals on the frame (ROI 1); a crystal that melts at 199 °C (ROI 2) and a crystal that melts at 203.5 °C (ROI 3)

can be explained by the fact that the liberation of water vapour during vaporization process could not be visually detected unless the sample was heated while immersed in silicone oil. The HSM light intensity profile of all crystals in the frame (ROI 1) presented in Fig. 9 shows that the responses to the thermal events that occurred below 170 °C were slightly disturbed by noise caused by the slight movement of some of the crystals, which has been observed to occur during heating. It is reported that besides an optical property change, a polymorphic transformation may also result in a movement of crystals since the transformation events may be accompanied by a change in volume of the crystals [47]. This observation demonstrates a limitation of the HSM light intensity profile in that it can be very sensitive to noise due to crystal movements.

Figure 11 compares the HSM light intensity profiles computed from three different ROIs: all crystals on the frame (ROI 1), a crystal that melts at 199 °C (ROI 2) and a crystal that melts at 203.5 °C (ROI 3). As was expected, ROI 2 does not show any light intensity change at 121 °C as detected by the DSC since the crystal should not undergo polymorphic transformation. Besides showing a sharp increase in the light intensity due to melting at 197.5 °C, ROI 2 also shows a sharp increase in the light intensity at 170.8 °C, which corresponds to a change in the crystal's optical property. This result implies that the change in optical property may not necessarily be due to the polymorphic transformation, but could also be due to a change in the surface property of the crystals due to the effect of increasing temperature. ROI 3, on the other hand, shows an increase in the light intensity profile at 165 °C, which is 5.8 °C lower than in ROI 2 but within the temperature range for transformation of form III to form I crystals (150–170 °C) reported in the literature [34]. It is therefore possible that the sharp increase in the HSM light intensity for ROI 2 and ROI 3 at 170.8 °C and 165 °C, respectively, was caused by two different events. ROI 3 also shows a change in the HSM light intensity due to melting at 203.5 °C, but the change shows a sharp decrease instead of a sharp increase. This peculiarity may be due to the presence of shadow, which darkens the selected region. However, in this case, only the change of the profile is of interest; the direction of the change is not important. The profiles of ROI 2 and ROI 3 seemed to be smoother compared to the profile of ROI 1. These results demonstrate that the HSM light intensity profile is strongly affected by the ROI sample location; the effect of noise and disturbances to the profile could be minimised through a proper selection of the ROI. The results of DSC and HSM with image analysis indicate that the sulfathiazole crystals obtained by method 3 initially comprised form II and form III crystals.

Crystals obtained by method 4

The results of the DSC and HSM analyses of the sulfathiazole crystals obtained using method 4 are presented in Fig. 12. Some images of the crystals during HSM analysis are shown in Fig. 13. The DSC curve indicates the presence of two endotherm peaks. The first peak maximum occurs at 142.5 °C whereas the second peak maximum occurs at 203 °C. The trend of the curve is in accordance with the results obtained by previous researchers [3, 34], in which the first peak was said to be due to the transformation of form IV into form I, whereas the second peak indicated the melting of form I. The HSM analysis confirmed that the first peak was not a melting peak since no melting was observed between 100 and 149 °C, as

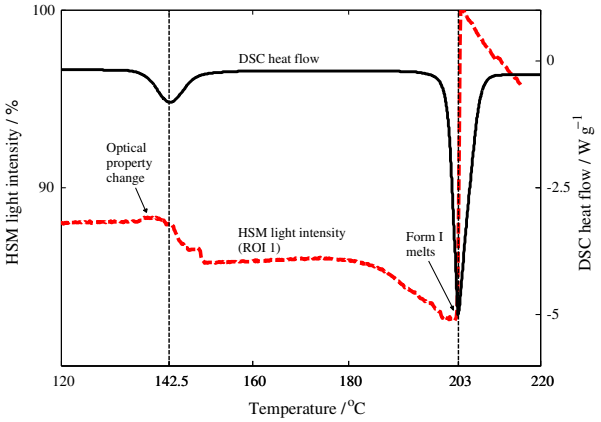

Fig. 12 DSC curve and HSM light intensity of sulfathiazole crystals obtained by method 4

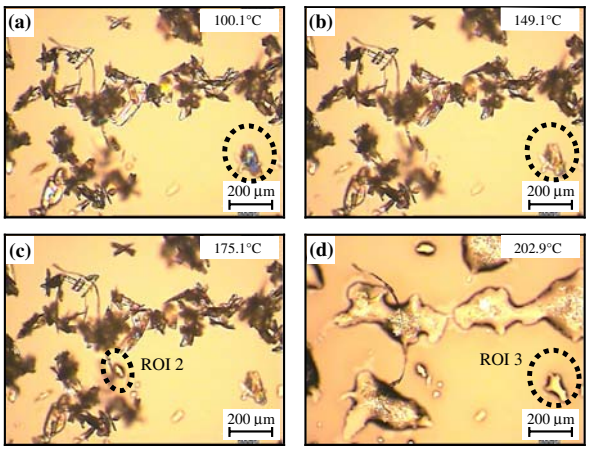

Fig. 13 Images of sulfathiazole crystals obtained by method 4 during HSM analysis taken at **a** 100.1 °C; **b** 149.1 °C; **c** 175.1 °C; and **d** 202.9 °C

indicated by the images of the crystals in Fig. 13a and b. There was, however, a change in the crystals' optical property as clearly shown by the difference in brightness of the highlighted crystals between (a) and (b) in Fig. 13. The HSM light intensity profile presented in Fig. 12 shows a decrease from 140 °C upwards until it stabilised above 150 °C. A slow decrease of light intensity value is shown from 180 °C until suddenly the value increased very fast starting from a temperature that corresponds to the melting of form I. The result signifies the capability of the light intensity profile to identify the beginning of the melting event earlier, since it is very sensitive to the changes happening on the surface of the crystals. The HSM analysis was able to detect a crystal that melts at 175.1 °C as shown by the highlighted crystal in Fig. 13c. It was not detected by either the DSC analysis or the HSM light intensity

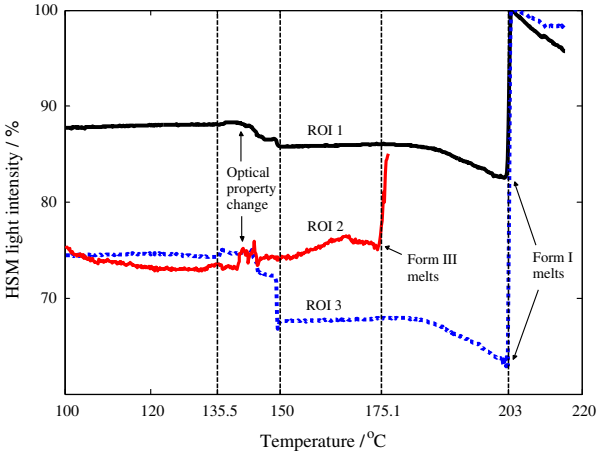

Fig. 14 HSM light intensity profiles of sulfathiazole crystals obtained by method 4 at three different ROIs; all crystals on the frame (ROI 1); a crystal that melts at 175.1 °C (ROI 2) and a crystal that melts at 203 °C (ROI 3)

profile computed from all crystals in the frame (ROI 1) presented in Fig. 12.

Figure 14 shows the HSM light intensity profiles computed from three different ROIs: all crystals on the frame (ROI 1); a crystal that melts at 175.1 °C (ROI 2), which is highlighted in Fig. 13c and a crystal that melts at 203 °C (ROI 3), which is highlighted in Fig. 13d. Generally, ROI 3 and ROI 1 are similar in the pattern of their profiles. This implies that most of the crystals in the sample had similar properties to the selected crystal in ROI 3. The profile of ROI 2 displays a sharp increase from 175.1 °C that corresponds to the melting of the crystal of form III. It also displays a slight fluctuation between 140 and 145 °C, but no significant decrease in light intensity was observed, which indicates the crystal did not undergo a polymorphic transformation. Despite its sensitivity to noise, the results illustrate the capability of the HSM light intensity to describe the thermal events of an individual crystal. The results of DSC and HSM with image analysis show that the sulfathiazole crystals obtained by method 4 initially contain crystals of form IV and a trace amount of form III.

Crystals obtained by method 5

Figure 15 shows the profiles of the DSC curve and the HSM light intensity of the crystals from method 5, while Fig. 16 shows the snapshots of the crystals during HSM analysis. The DSC curve indicates the presence of three major endotherm peaks. The first peak at a maximum of 161 °C corresponds to a change in the optical properties of the crystals. This is verified by the HSM analysis as shown by the difference in the brightness of the highlighted crystals between Fig. 16a and b. As mentioned previously,

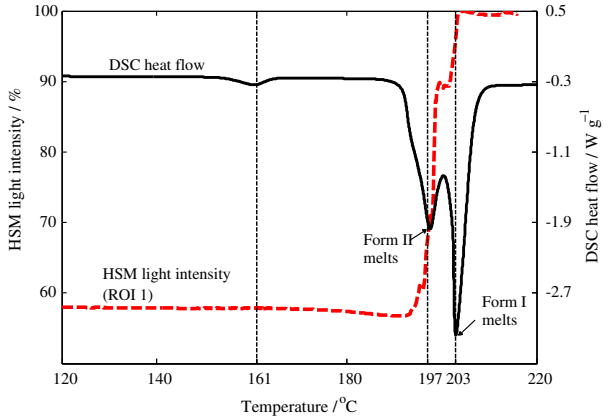

Fig. 15 DSC curve and HSM light intensity of sulfathiazole crystals obtained by method 5

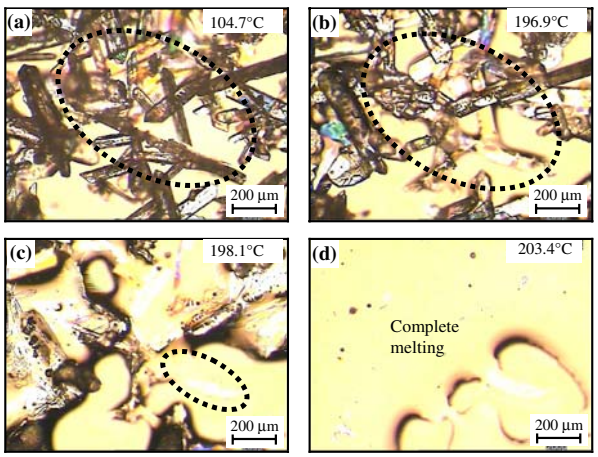

Fig. 16 Images of sulfathiazole crystals obtained by method 5 during HSM analysis taken at **a** 104.7 °C; **b** 196.9 °C; **c** 198.1 °C; and **d** 203.4 °C

a peak formation in a temperature range of 150–170 °C may be due to a transformation of form III to form I. However, the HSM light intensity profile computed from all the crystals on the frame (ROI 1) presented in Fig. 15 does not show any change in optical property of the crystals. This may be due to the averaging-out effect that makes the event undetectable in the HSM light intensity profile. The melting of the crystals at 197 and 203 °C are illustrated by the HSM light intensity profile in Fig. 15 as two consecutive sharp increases.

Figure 17 compares the HSM light intensity profiles between the one computed from all crystals in the frame (ROI 1) with another from a crystal that melts at 197 °C (ROI 2) as highlighted in Fig. 16c. The HSM light intensity profile of ROI 2 differentiates itself from the profile of ROI 1 by not indicating melting at 203 °C. The results signify the potential of the HSM light intensity profile to provide a

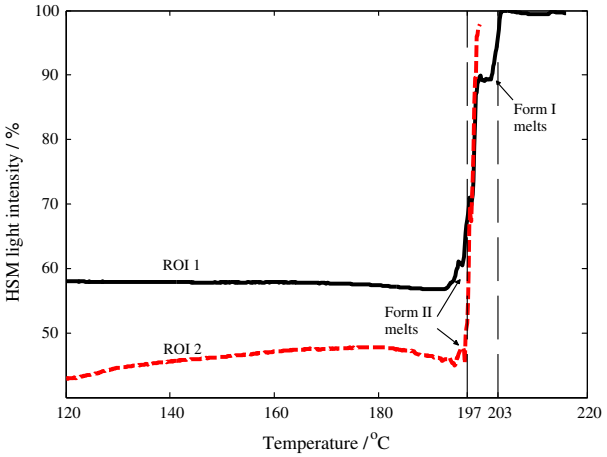

Fig. 17 HSM light intensity profiles of sulfathiazole crystals obtained by method 5 at three different ROIs; all crystals on the frame (ROI 1); a crystal that melts at 197 °C (ROI 2) and a crystal that melts at 203 °C (ROI 3)

unique description of the changes happening to individual crystals. The results of a combined approach of DSC and HSM with image analysis show that the sulfathiazole crystals obtained by method 5 initially contain crystals of form II and form III.

Conclusions

The crystallisation of sulfathiazole polymorphs was investigated by a combined DSC-HSM with image analysis approach. The approach provides synergistic benefits of two characterisation techniques and the use of image analysis gives a unique insight into the thermal behaviour of the polymorphic system. The capability of the HSM image analysis to provide alternative and quantitative ways of presenting the HSM results has been demonstrated. It translates visual effects, which other characterisation techniques may not be able to provide, into quantitative information. Despite its sensitivity to noise, the light intensity profile obtained from HSM image analysis was found to be capable of describing thermal behaviour of individual crystals and very sensitive to the changes happening on the surface of these crystals. With these unique capabilities, the HSM image analysis allows verification of thermal events, particularly in confirming the formation of mixtures of polymorphs. The results of the experiments showed that, although the methods to produce pure polymorphs were used, most of the time sulfathiazole crystallised as mixtures of polymorphs.

Acknowledgements The authors thank Dr. David Ross of the Department of Materials, Loughborough University for the use of the HSM system. Financial support provided by the Engineering and

Physical Sciences Research Council (EPSRC), U.K., (grant EP/E022294/1) is gratefully acknowledged. One of the authors (MRAB) is grateful to the Malaysian Ministry of Higher Education and the International Islamic University Malaysia for a scholarship.

References

1. Karpinski PH. Polymorphism of active pharmaceutical ingredients. Chem Eng Technol. 2006;29:233–7.
2. Hilfiker R, Blatter F, von Raumer M. Relevance of solid-state properties for pharmaceutical products. In: Hilfiker R, editor. Polymorphism in the pharmaceutical industry. Weinheim: Wiley-VCH Verlag GmbH & Co; 2006. p. 1–18.
3. Kordikowski A, Shekunov T, York P. Polymorph control of sulfathiazole in supercritical CO_2. Pharm Res. 2001;18:682–8.
4. Pollanen K, Hakkinen AW, Reinikainen SP, Louhi-Kultanen A, Nystrom L. A study on batch cooling crystallization of sulphathiazole—process monitoring using ATR-FTIR and product characterization by automated image analysis. Chem Eng Res Des. 2006;84:47–59.
5. Abu Bakar MR, Nagy ZK, Saleemi AN, Rielly CD. The impact of direct nucleation control on crystal size distribution in pharmaceutical crystallization processes. Cryst Growth Des. 2009;9:1378–84.
6. Woo XY, Nagy ZK, Tan RBH, Braatz RD. Adaptive concentration control of cooling and antisolvent crystallization with laser backscattering measurement. Cryst Growth Des. 2009;9:182–91.
7. Nagy ZK, Chew JW, Fujiwara M, Braatz RD. Comparative performance of concentration and temperature controlled batch crystallizations. J Process Control. 2008;18:399–407.
8. Craig DQM, Reading M. Thermal analysis of pharmaceuticals. Boca Raton, USA: CRC Press; 2007.
9. Barnes AF, Hardy MJ, Lever TJ. A review of the applications of thermal methods within the pharmaceutical industry. J Therm Anal. 1993;40:499–509.
10. Giron D. Applications of thermal analysis in the pharmaceutical industry. J Pharm Biomed Anal. 1986;4:755–70.
11. Giron D. Thermal analysis and calorimetric methods in the characterization of polymorphs and solvates. Thermochim Acta. 1995;248:1–59.
12. Giron D. Contribution of thermal methods and related techniques to the rational development of pharmaceuticals—part 1. PSTT. 1998;1:191–9.
13. Reading M, Craig DQM. Principles of differential scanning calorimetry. In: Craig DQM, Reading M, editors. Thermal analysis of pharmaceuticals. Boca Raton, USA: CRC Press; 2007. p. 1–20.
14. Clas S-D, Dalton CR, Hancock BC. Differential scanning calorimetry: applications in drug development. PSTT. 1999;2:311–20.
15. Vitez IM, Newman AW, Davidovich M, Kiesnowski C. The evolution of hot-stage microscopy to aid solid-state characterizations of pharmaceutical solids. Thermochim Acta. 1998;324:187–96.
16. Marthi K, Ács M, Pokol G, Tomor K, Eröss-Kiss KJ. DSC studies on the polymorphism and pseudopolymorphism of pharmaceutical substances: A complex system for studying physico-chemical behaviour of binary mixtures. J Therm Anal. 1992;38:1017–25.
17. Vitez IM, Newman AW. Thermal microscopy. In: Craig DQM, Reading M, editors. Thermal analysis of pharmaceuticals. Boca Raton, USA: CRC Press; 2007. p. 221–64.
18. Patience DB, Dell'Orco PC, Rawlings JB. Optimal operation of a seeded pharmaceutical crystallization with growth-dependent dispersion. Org Proc Res Dev. 2004;8:609–15.
19. Calderon De Anda J, Wang XZ, Roberts KJ. Multi-scale segmentation image analysis for the in-process monitoring of particle shape with batch crystallisers. Chem Eng Sci. 2005;60:1053–65.
20. Wang XZ, Roberts KJ, Ma C. Crystal growth measurement using 2D and 3D imaging and the perspectives for shape control. Chem Eng Sci. 2008;63:1173–84.
21. Simon LL, Nagy ZK, Hungerbuehler K. Comparison of external bulk video imaging with focused beam reflectance measurement and ultra-violet visible spectroscopy for metastable zone identification in food and pharmaceutical crystallization processes. Chem Eng Sci. 2009;64:3344–51.
22. Simon LL, Nagy ZK, Hungerbuehler K. Endoscopy-based in situ bulk video imaging of batch crystallization processes. Org Proc Res Dev. 2009; 6. doi:10.1021/op900019b.
23. Giron D. Investigations of polymorphism and pseudo-polymorphism in pharmaceuticals by combined thermoanalytical techniques. J Therm Anal Calorim. 2001;64:37–60.
24. Giron D. Applications of thermal analysis and coupled techniques in pharmaceutical industry. J Therm Anal Calorim. 2002;68:335–57.
25. Pommerenke K. DSC and thermomicroscopy combined. Am Lab. 2000;32:30–2.
26. Richardson MF, Yang Q-C, Novotny-Bregger E, Dunitz JD. Conformational polymorphism of dimethyl 3,6-dichloro-2,5-dihydroxyterephthalate. II. Structural, thermodynamic, kinetic and mechanistic aspects of phase transformations among the three crystal forms. Acta Crystallogr. 1990;B46:653–60.
27. Wiedemann HG, Bayer G. Application of simultaneous thermomicroscopy/DSC to the study of phase diagrams. J Therm Anal. 1985;30:1273–81.
28. Wiedemann HG, Felder-Casagrande S. Thermomicroscopy. In: Brown ME, editor. Handbook of thermal analysis and calorimetry. Vol. 1: Principles and practice. Elsevier Science B.V.: Amsterdam; 1998. p. 473–96.
29. da Silva RMF, De Medeiros FPM, Nascimento TG, Macedo RO, Neto PJR. Thermal characterization of indinavir sulfate using TG, DSC and DSC-photovisual. J Therm Anal Calorim. 2009;95:965–8.
30. Apperley DC, Fletton RA, Harris RK, Lancaster RW, Tavener S, Threlfall TL. Sulfathiazole polymorphism studied by magic-angle Spinning NMR. J Pharm Sci. 1999;88:1275–80.
31. Chan FC, Anwar J, Cernik R, Barnes P, Wilson RM. Ab initio structure determination of sulfathiazole polymorph V from synchrotron X-ray powder diffraction data. J Appl Crystallogr. 1999;32:436–41.
32. Hughes DS, Hursthouse MB, Threlfall T, Tavener S. A new polymorph of sulfathiazole. Acta Crystallogr C. 1999;55:1831–3.
33. Blagden N, Davey RJ, Lieberman HF, Williams L, Payne R, Roberts R, et al. Crystal chemistry and solvent effects in polymorphic systems: sulfathiazole. J Chem Soc, Faraday Trans. 1998;94: 1035–44.
34. Anwar J, Tarling SE, Barnes P. Polymorphism of sulphathiazole. J Pharm Sci. 1989;78:337–42.
35. Lagas M, Lerk CF. The polymorphism of sulphathiazole. Int J Pharm. 1981;8:25–33.
36. Mesley RJ. The polymorphism of sulfathiazole. J Pharm Pharm. 1971;23:687–94.
37. Hughes DS, Hursthouse MB, Lancaster RW, Tavener S, Threlfall T, Turner P. How many polymorphs has sulfathiazole? Proposals for reporting crystallographic data of polymorphs. J Pharm Pharm. 1997;49:20.
38. Anderson JE, Moore S, Tarczynski F, Walker D. Determination of the onset of crystallization of N1-2-(thiazolyl)sulfanilamide (sulfathiazole) by UV-Vis and calorimetry using an automated reaction platform; subsequent characterization of polymorphic forms using dispersive Raman spectroscopy. Spectrochim Acta A. 2001;57:1793–808.

39. Aaltonen J, Rantanen J, Siiria S, Karjalainen M, Jorgensen A, Laitinen N, et al. Polymorph screening using near-infrared spectroscopy. Anal Chem. 2003;75:5267–73.
40. Hakkinen A, Pollanen K, Karjalainen M, Rantanen J, Louhi-Kultanen M, Nystrom L. Batch cooling crystallization and pressure filtration of sulphathiazole: the influence of solvent composition. Biotechnol Appl Biochem. 2005;41:17–28.
41. Khoshkhoo S, Anwar J. Crystallization of polymorphs: the effect of solvent. J Phys D. 1993;26:B90–3.
42. Gelbrich T, Hughes DS, Hursthouse MB, Threlfall TL. Packing similarity in polymorphs of sulfathiazole. Cryst Eng Comm. 2008;10:1328–34.
43. Lever T. Optimizing DSC experiments. In: Craig DQM, Reading M, editors. Thermal analysis of pharmaceuticals. Boca Raton, USA: CRC Press; 2007. p. 24–51.
44. Urakami K, Shono Y, Higashi A, Umemoto K, Godo M. Estimation of transition temperature of pharmaceutical polymorphs by measuring heat of solution and solubility. Bull Chem Soc Jpn. 2002;75:1241–5.
45. Miller RP, Sommer G. A hot stage microscope incorporating a differential thermal analysis unit. J Sci Instrum. 1966;43:293–7.
46. Howard KS, Nagy ZK, Saha B, Robertson AL, Steele G. Combined PAT-solid state analytical approach for the detection and study of sodium benzoate hydrate. Org Proc Res Dev. 2009; 13:590–7.
47. Warrington SB. Simultaneous thermal analysis techniques. In: Haines PJ, editor. Principles of thermal analysis and calorimetry. Cambridge: The Royal Society of Chemistry; 2002. p. 166–89.